Quantitative Orientation Measurements in Thin Lipid Films by Attenuated Total Reflection Infrared Spectroscopy

Frédéric Picard,* Thierry Buffeteau,# Bernard Desbat,# Michèle Auger,* and Michel Pézolet*
*Département de Chimie, Centre de Recherche en Sciences et Ingénierie des Macromolécules, Université Laval, Québec, Québec, Canada G1K 7P4, and #Laboratoire de Physico-Chimie Moléculaire (U.M.R. 5803), 33405 Talence, France

ABSTRACT Quantitative orientation measurements by attenuated total reflectance (ATR) infrared spectroscopy require the accurate knowledge of the dichroic ratio and of the mean-square electric fields along the three axes of the ATR crystal. In this paper, polarized ATR spectra of single supported bilayers of the phospholipid dimyristoylphosphatidic acid covered by either air or water have been recorded and the dichroic ratio of the bands due to the methylene stretching vibrations has been calculated. The mean-square electric field amplitudes were calculated using three formalisms, namely the Harrick thin film approximation, the two-phase approximation, and the thickness- and absorption-dependent one. The results show that for dry bilayers, the acyl chain tilt angle varies with the formalism used, while no significant variations are observed for the hydrated bilayers. To test the validity of the different formalisms, s- and p-polarized ATR spectra of a 40-Å lipid layer were simulated for different acyl chain tilt angles. The results show that the thickness- and absorption-dependent formalism using the mean values of the electric fields over the film thickness gives the most accurate values of acyl chain tilt angle in dry lipid films. However, for lipid monolayers or bilayers, the tilt angle can be determined with an acceptable accuracy using the Harrick thin film approximation. Finally, this study shows clearly that the uncertainty on the determination of the tilt angle comes mostly from the experimental error on the dichroic ratio and from the knowledge of the refractive index.

INTRODUCTION

Fourier transform infrared (FTIR) spectroscopy has been widely used for the study of biological molecules (Mantsch and Chapman, 1996) since the shape, intensity, and position of infrared bands are sensitive to the structure and motion of the molecular species. In addition, due to the fact that the absorption of the infrared radiation depends on the angle between the polarization of the incident radiation and the transition moment of a given vibration, it is also possible to characterize the molecular orientation in samples deposited on different types of substrates by means of polarized FTIR spectroscopy. For that purpose, different techniques have been used, namely polarized transmission spectroscopy (Rothschild and Clark, 1979; Chollet and Messier, 1982; Vogel et al., 1983), infrared reflection absorption spectroscopy (IRRAS) (Allara and Swallen, 1982; Rabolt et al., 1983; Umemura et al., 1990; Blaudez et al., 1998), polarization-modulation (PM) IRRAS (Golden et al., 1981; Buffeteau et al., 1991; Blaudez et al., 1993), and polarized attenuated total reflection (ATR) spectroscopy (Harrick, 1967; Fringeli and Günthard, 1981; Kimura et al., 1986; Ahn and Franses, 1992). ATR spectroscopy is a very effective technique for studying biological materials because the sample can be readily oriented on the ATR crystal and kept in an aqueous environment. This sampling technique has been used extensively to study proteins (Goormaghtigh et al., 1990), phospholipid multilayers and monolayers (Fringeli and Günthard, 1981; Okamura et al., 1985; Brandenburg and Seydel, 1986; Lotta et al., 1988), lipid-protein complexes (Okamura et al., 1986; Brauner et al., 1987; Cornell et al., 1989; Frey and Tamm, 1991; Subirade et al., 1995; Axelsen et al., 1995a), and membrane receptors (Baenziger et al., 1992). Even though polarized transmission and IRRAS results can be interpreted in a straightforward manner, it is not the case for ATR spectroscopy, since the electric field amplitudes of the infrared evanescent wave along the three coordinates of the ATR crystal have to be calculated to determine the order parameter from the linear dichroism of the infrared bands (Harrick, 1967; Mirabella and Harrick, 1985).

Some thirty years ago, Harrick (1967) derived analytical equations to calculate these electric field amplitudes for the limiting cases known as the thin-film approximation and the thick-film approximation. According to the Harrick thin-film approximation, the film thickness is very small compared to the penetration depth of the evanescent wave and the electric field amplitudes calculated are those at the surface of the ATR crystal. Thin films of phospholipids and proteins deposited either by the Langmuir-Blodgett technique (Lukes et al., 1992; Axelsen et al., 1995a, b; Subirade et al., 1995), by evaporation from organic solvent (Fringeli and Günthard, 1981; Brauner et al., 1987), or by fusion of small unilamellar vesicles of phospholipids (Frey and Tamm, 1991) have often been considered as Harrick thin films.

Recently, the thin film approximation has been questioned because it failed to give reliable results concerning the orientation of the helical polypeptides poly-γ-benzyl-L-glutamate and poly-β-benzyl-L-aspartate, and the bee venom toxin melittin (Citra and Axelsen, 1996). It was then

Received for publication 18 May 1998 and in final form 24 August 1998.
Address reprint requests to Michel Pézolet, Département de Chimie, CERSIM, Université Laval, Québec, Québec, Canada G1K 7P4. Tel.: 418-656-2481; Fax: 418-656-7916; E-mail: Michel.Pezolet@chm.ulaval.ca.

0006-3495/99/01/539/13 $2.00

proposed that for very thin films, such as supported lipid monolayers and bilayers, the optical constants of the film are highly perturbed by the optical properties of the adjacent media and that the optical properties of the film should be neglected. This model, named the two-phase approximation (Citra and Axelsen, 1996), had already been used in the literature by other investigators (Higashiyama and Takenaka, 1974; Takenaka et al., 1980; Cropek and Bohn, 1990; Jang and Miller, 1995). With the two-phase approximation, Citra and Axelsen (1996) have obtained good results for the orientation of poly-γ-benzyl-glutamate deposited on a hydrophobic substrate that were in agreement with those obtained by other spectroscopic techniques. In addition, this approach seems to eliminate the divergence between the results obtained in the controversial case of melittin bound to lipid membranes (Vogel et al., 1983; Brauner et al., 1987; Frey and Tamm, 1991). However, the Harrick thin film approximation has been used successfully for orientation measurements of dry phospholipid monolayers (Subirade et al., 1995; Labrecque, 1995) and for the orientation of dimyristoylphosphatidylcholine (DMPC) in supported DMPC-gramicidin monolayers deposited on a hydrophobic crystal covered with water (Axelsen et al., 1995a).

The origin of the problems encountered with quantitative orientation measurements using polarized ATR spectroscopy may come from the miscalculation of the mean-square electric field amplitudes. As pointed out recently by Axelsen and Citra (1997), the electric field amplitudes may not be suitably calculated from the Harrick thin film equations. These equations are approximate and do not take into account the film thickness and the absorption of the different media. A wrong evaluation of the physical properties of the film, such as the refractive index or the thickness (thin or thick films) may also lead to the miscalculation of the electric fields. It has also been suggested that the optical properties of an ultra-thin film, and consequently the electric field amplitudes in the film, may be modified by the adjacent media (Axelsen and Citra, 1997).

To address these problems, we have made a detailed analysis of the ATR spectra of supported single bilayers of dimyristoylphosphatidic acid (DMPA) covered by either air or water. A phospholipid has been chosen since it is well known that phospholipids can form highly oriented bilayers whose orientation has been studied by x-ray diffraction (Harlos et al., 1984; Pascher et al., 1987). In addition, the acyl chains for lipid bilayers in the gel phase are in the all-*trans* conformation and the transition moments of the methylene stretching vibrations are perpendicular to the chain axis. In the present study, DMPA was in part chosen because of its high gel-to-liquid crystalline phase transition temperature (48°C) (Van Dick et al., 1978). Therefore, the spectra obtained at room temperature (~25°C below the phase transition temperature) should be representative of lipids in the gel phase.

The anisotropic optical constants (real refractive index and extinction coefficient in and out of the plane of the film) were first determined from the polarized ATR spectra. Then, the mean-square electric field amplitudes along the three axes of the ATR crystal were calculated using a matricial formalism (Hansen, 1965, 1968, 1972, 1973) that takes into account the number of layers, their complex refractive index, and their thickness. These electric field amplitudes were then compared with those calculated from the Harrick thin film equations and from the two-phase approximation. To test the validity of the different models used to calculate the mean-square electric field amplitudes, s- and p-polarized ATR spectra of a 40-Å lipid layer were simulated for different molecular tilt angles. For each spectrum simulated with a given tilt angle ("real tilt angle"), we have calculated the dichroic ratio and the associated order parameter and tilt angle ("calculated tilt angle"). The difference between the real and calculated tilt angles has been analyzed to determine which model gives better values of the electric field amplitudes. Finally, the different factors affecting the orientation measurements have been analyzed.

THEORY

The computer programs developed to calculate the ATR spectra of multilayer systems and the intensity of the electric fields in each layer use the Abelès's matricial formalism (Abelès, 1967). This formalism is based on the fact that the equations that govern the propagation of light are linear and that the continuity of the tangential fields across an interface between two isotropic media can be regarded as a 2×2 linear matrix transformation. In this section, the complex refractive index, $\hat{n}_j$, is defined as follows:

$$\hat{n}_j = n_j + ik_j \tag{1}$$

where i is equal to $\sqrt{-1}$, n_j is the refractive index, and k_j is the extinction coefficient of the jth layer.

Spectral simulation

In the Abelès's matrical formalism, the relationship between the components of the electric (E) and magnetic (H) field vectors at the upper and lower sides of the jth layer is governed by the characteristic matrix (Hansen, 1968):

$$M_j = \begin{bmatrix} \cos\beta_j & \dfrac{-i\sin\beta_j}{g_j} \\ -i\,g_j\sin\beta_j & \cos\beta_j \end{bmatrix} \tag{2}$$

where $\beta_j = 2\pi d_j \hat{n}_j \cos\phi_j/\lambda$ represents the phase thickness, $g_j = \cos\phi_j/\hat{n}_j$ for p polarization (electric field vector parallel to the plane of incidence, which is defined by the (x, z) plane), and $g_j = \hat{n}_j \cos\phi_j$ for s polarization (electric field vector perpendicular to the plane of incidence, along the y axis).

In these terms, λ is the wavelength of the incident light in vacuum, d_j is the thickness of the jth layer, and ϕ_j is the angle of refraction in layer j; ϕ_j is related to the incidence angle ϕ_1 by Snell's law and satisfies $n_1 \sin\phi_1 = \hat{n}_j \sin\phi_j$.

The two tangential fields at the first boundary are related to those at the final boundary by

$$\begin{bmatrix} U_1 \\ V_1 \end{bmatrix} = M_2 M_3 \ldots M_{N-1} \begin{bmatrix} U_{N-1} \\ V_{N-1} \end{bmatrix}$$

$$= M \begin{bmatrix} U_{N-1} \\ V_{N-1} \end{bmatrix} = \begin{bmatrix} m_{11} & m_{12} \\ m_{21} & m_{22} \end{bmatrix} \begin{bmatrix} U_{N-1} \\ V_{N-1} \end{bmatrix} \quad (3)$$

where M is the characteristic matrix of an N phase system (i.e., N − 2 layers between semi-infinite initial ($j = 1$) and final ($j = N$) phases), and U_k and V_k are the tangential components of the field amplitudes at the boundary k. $U_k = E_{yk}$ and $V_k = H_{xk}$ for s polarization while $U_k = H_{yk}$ and $V_k = E_{xk}$ for p polarization.

With the use of the components of M, the reflection coefficients of the multilayer system are expressed, for each polarization, as follows:

$$\hat{r} = \frac{(m_{11} + m_{12} g_N) g_1 - (m_{21} + m_{22} g_N)}{(m_{11} + m_{12} g_N) g_1 + (m_{21} + m_{22} g_N)}. \quad (4)$$

The polarized and unpolarized reflectances, which can be directly measured, are given by

$$R_s = |\hat{r}_s|^2 \quad R_p = |\hat{r}_p|^2 \quad \text{and} \quad R = \frac{R_s + R_p}{2}. \quad (5)$$

As a result, ATR spectra for a multilayer system can be simulated considering the first phase as the denser medium (refractive index of the crystal) and knowing the complex refractive index and the thickness of each layer. It should be mentioned that the matrix method can be generalized for anisotropic layers, as shown by Yamamoto and Ishida (1994). In this case, $\hat{n}_j$ must be replaced by $\hat{n}_{yj}$ and $\hat{n}_{xj}$ for s and p polarizations, respectively. However, the Snell's law for p polarization becomes $n_1 \sin \phi_1 = \hat{n}_{zj} \sin \phi_j$.

Mean-square electric field amplitudes

Thickness- and absorption-dependent equations

The general procedure for calculating electric field components at any point in an isotropic stratified system is well developed by Hansen (1968), and is briefly summarized below.

The two tangential field components at point z in phase k are given by

$$\begin{bmatrix} U_k(z) \\ V_k(z) \end{bmatrix} = M_k^{-1}(z) \prod_{j=k-1}^{2} M_j^{-1} \begin{bmatrix} U_1 \\ V_1 \end{bmatrix} \quad (6)$$

where M_j^{-1} are the inverse matrices of M_j, and are obtained by changing the sign of the m_{12} and m_{21} elements in Eq. 2.

For s polarization, the tangential fields at the first interface are

$$\begin{bmatrix} U_1 \\ V_1 \end{bmatrix} = \begin{bmatrix} E_{y1} \\ H_{x1} \end{bmatrix} = \begin{bmatrix} 1 + \hat{r}_s \\ -g_1(1 - \hat{r}_s) \end{bmatrix}.$$

Equation 6 can be written as follows:

$$\begin{bmatrix} E_{yk(z)} \\ H_{xk}(z) \end{bmatrix} = \begin{bmatrix} m_{11}(z) & -m_{12}(z) \\ -m_{21}(z) & m_{22}(z) \end{bmatrix} \cdot \begin{bmatrix} 1 + \hat{r}_s \\ -g_1(1 - \hat{r}_s) \end{bmatrix}. \quad (7)$$

where $m_{11}(z)$, $m_{12}(z)$, $m_{21}(z)$, and $m_{22}(z)$ are the elements of the $M_k^{-1}(z) \prod_{j=k-1}^{2} M_j^{-1}$ matrix.

The mean-square electric field along y is given by

$$\langle E_{yk}^2(z) \rangle = |m_{11}(z)(1 + \hat{r}_s) + m_{12}(z) g_1 (1 - \hat{r}_s)|^2. \quad (8)$$

For p polarization, the tangential fields at the first interface are

$$\begin{bmatrix} U_1 \\ V_1 \end{bmatrix} = \begin{bmatrix} H_{y1} \\ E_{x1} \end{bmatrix} = n_1 \begin{bmatrix} 1 + \hat{r}_p \\ -g_1(1 - \hat{r}_p) \end{bmatrix}.$$

The mean-square electric field along x is given by

$$\langle E_{xk}^2(z) \rangle = n_1^2 |-m_{21}(z)(1 + \hat{r}_p) - m_{22}(z) g_1 (1 - \hat{r}_p)|^2. \quad (9)$$

The electric field along z, E_{zk} can be derived from the magnetic field H_{yk} by the relation

$$E_{zk} = \frac{n_1 \sin \phi_1 H_{yk}}{n_k^2} \quad (10)$$

and the mean-square electric field along z is given by

$$\langle E_{zk}^2(z) \rangle = n_1^4 \sin^2 \phi_1 \left| \frac{m_{11}(z)(1 + \hat{r}_p) + m_{12} g_1 (1 - \hat{r}_p)}{\hat{n}_k^2} \right|^2, \quad (11)$$

The explicit expressions of the mean-square electric field amplitudes can be obtained through pure geometrical optics (Hansen, 1968) or derived from Eqs. 8, 9, and 11 for a two-, three-, and four-phase stratified system (Axelsen and Citra, 1997). These expressions are called thickness- and absorption-dependent expressions since they take into account the thickness and the absorption properties of the intermediate phases.

Approximate equations (Harrick equations)

A set of approximate equations for the mean-square electric field amplitudes in the second phase of a two-phase system were first proposed by Harrick (1965). These equations, called the two-phase approximation, are obtained from the thickness- and absorption-dependent expressions by setting $z = 0$ and are given by

$$\langle E_{x2}^2(0) \rangle = \frac{4 \cos^2 \phi_1 (\sin^2 \phi_1 - n_{21}^2)}{(1 - n_{21}^2)[(1 + n_{21}^2) \sin^2 \phi_1 - n_{21}^2]} \quad (12)$$

$$\langle E_{y2}^2(0) \rangle = \frac{4 \cos^2 \phi_1}{(1 - n_{21}^2)} \quad (13)$$

$$\langle E_{z2}^2(0) \rangle = \frac{4 \cos^2 \phi_1 \sin^2 \phi_1}{(1 - n_{21}^2)[(1 + n_{21}^2) \sin^2 \phi_1 - n_{21}^2]} \quad (14)$$

In these equations ϕ_1 is the incidence angle in the ATR crystal and $n_{21} = n_2/n_1$, where n_1 and n_2 are the real parts of the refractive indexes of phase 1 (ATR crystal) and phase 2 (semi-infinite nonabsorbing phase). These equations can be used for a three-phase system when the thickness of the layer (phase 2) is very large compared to the depth of penetration, d_p, defined by

$$d_p = \frac{\lambda}{2\pi n_1(\sin^2\phi_1 - n_{21}^2)^{1/2}}, \tag{15}$$

Harrick has also proposed approximate equations for calculating the mean-square electric field amplitudes when the thickness of the layer is very small compared to the depth of penetration (Harrick, 1967). These equations, called the thin film approximation, are given by

$$\langle E_{x2}^2(0)\rangle = \frac{4\cos^2\phi_1(\sin^2\phi_1 - n_{31}^2)}{(1 - n_{31}^2)[(1 + n_{31}^2)\sin^2\phi_1 - n_{31}^2]} \tag{16}$$

$$\langle E_{y2}^2(0)\rangle = \frac{4\cos^2\phi_1}{(1 - n_{31}^2)} \tag{17}$$

$$\langle E_{z2}^2(0)\rangle = \frac{4n_{32}^4\cos^2\phi_1\sin^2\phi_1}{(1 - n_{31}^2)[(1 + n_{31}^2)\sin^2\phi_1 - n_{31}^2]} \tag{18}$$

where $n_{31} = n_3/n_1$ and $n_{32} = n_3/n_2$.

Determination of the optical constants of a uniaxial ultrathin film

A method for the determination of the optical constants of a uniaxial film ($n_x = n_y$, n_z and $k_x = k_y$, k_z) has recently been described (Buffeteau et al., 1997). In this method, the optical constants in the plane ($n_x = n_y$ and $k_x = k_y$) of the thin film deposited onto a transparent substrate (calcium fluoride, zinc selenide, silicon ...) are determined from its transmittance spectrum at normal incidence. However, the optical constants perpendicular to the plane of the thin film (n_z and k_z) are determined from its p-polarized reflectance spectrum at grazing incidence ($\phi_1 = 85°$) on a metallic substrate (IRRAS spectrum). Although this approach gives good results for ultrathin films, it requires that the molecular orientation is the same on all substrates used. In the current study, we have used a new method where the optical constants are determined directly from the s- and p-polarized ATR spectra (T. Buffeteau, unpublished results). The main advantage of this method is that all measurements are performed on the same sample.

A first estimation of the optical constants can be obtained using approximate equations of ATR spectra of ultrathin films in air ($n_3 = 1$). Indeed, using the thin film approximation ($d \ll \lambda$), the s-polarized ATR spectrum is given by

$$\frac{R_s(d)}{R_s(0)} = 1 - \frac{8\pi d n_1\cos\phi_1}{\lambda(n_1^2 - 1)}\,\mathrm{Im}(\hat{\epsilon}_y) \tag{19}$$

and the p-polarized ATR spectrum is given by

$$\frac{R_p(d)}{R_p(0)} = 1 - \frac{8\pi d n_1\cos\phi_1}{\lambda[\cos^2\phi_1 - n_1^2(1 - n_1^2\sin^2\phi_1)]} \cdot \left[(n_1^2\sin^2\phi_1 - 1)\mathrm{Im}(\hat{\epsilon}_x) + n_1^2\sin^2\phi_1\mathrm{Im}\left(-\frac{1}{\hat{\epsilon}_z}\right)\right] \tag{20}$$

where $R_{s,p}(d)$ and $R_{s,p}(0)$ are the s- and p-polarized single reflection ATR spectra for the covered and uncovered crystal, respectively; n_1 is the refractive index of the ATR crystal, and $\hat{\varepsilon} = \hat{n}^2$ is the complex dielectric constant of the film.

Equation 19 can be used to extract the imaginary part of the dielectric function $\hat{\varepsilon}_y = \hat{\varepsilon}_x$, and its real part can be calculated by Kramers-Kronig transformation of the imaginary part. Then, the initial real and imaginary parts of the dielectric function are used for calculating the s-polarized ATR spectrum and are perturbed by a Newton-Raphson method until the simulated and experimental spectra are sufficiently close to each other. Finally, the in-plane optical constants are calculated by simple arithmetical equations using the real and the imaginary parts of the dielectric function.

To calculate the optical constants perpendicular to the plane of the film from the p-polarized ATR spectrum, the imaginary part of $(-1/\hat{\varepsilon}_z)$ is first calculated using Eq. 20 with the value of the dielectric function $\hat{\varepsilon}_y = \hat{\varepsilon}_x$ obtained from the s-polarized ATR spectrum. Then, the same procedure as above is used to determine the final values of the out-of-plane optical constants.

MATERIALS AND METHODS

Materials

The sodium salt of dimyristoylphosphatidic acid (DMPA) was obtained from Avanti Polar Lipids (Alabaster, AL) and used without further purification. The water used throughout this study was demineralized and deionized using a Barnstead NANOpurII system (Boston, MA) with four purification columns.

Sample preparation

The pH of the water used for all the experiments was adjusted to 6.5 with diluted NaOH using a microelectrode (Microelectrodes, Inc., Londonderry, NH). An aqueous dispersion of DMPA (2% wt/wt) was prepared by mixing the appropriate amount of solid in water. This dispersion was then heated to ~65°C for 10 min, stirred on a vortex mixer, and cooled down to 0°C for 10 min. This cycle was repeated at least five times to obtain multilamellar vesicles (MLV). Supported lipid bilayers were prepared by condensing small unilamellar vesicles (SUV) on the germanium ATR crystal as described previously for silica beads (Bayerl and Bloom, 1990; Picard et al., 1998). The SUV were prepared by extruding the MLV dispersion three times through a 0.1 μm polycarbonate filter (Nucleopore, Toronto, ON) at a temperature above the lipid gel-to-liquid crystalline phase transition temperature using a Lipex extruder (Vancouver, BC). The SUV were then diluted to obtain a lipid concentration of 1% (wt/wt). The lipid solution was then heated to 65°C and the ATR crystal was immersed in it

for 15 min. The solution was cooled down below the lipid phase transition temperature (48°C) and the ATR crystal was pulled out and immersed twice in pure water to eliminate the excess of lipid. The single bilayers so obtained on each side of the ATR crystal were dried out with a gentle nitrogen stream.

FTIR measurements

Infrared spectra were recorded at room temperature (21°C) on a Nicolet Magna 550 (Madison, WI) Fourier transform infrared spectrometer equipped with a narrow-band mercury-cadmium-telluride detector and a germanium-coated KBr beamsplitter. A total of 1000 scans were averaged at 2 cm^{-1} resolution after triangular apodization. For polarization measurements, the infrared radiation was polarized with a ZnSe wire-grid polarizer (Specac, Orpington, UK).

A bilayer was deposited on the two sides of a germanium ATR plate (50 × 20 × 2 mm, 45° parallelogram, 24 reflections). Prior to the deposition, the germanium crystal was cleaned with ethanol and water and placed for 5 min in a plasma cleaner (Harrick, NY). The crystal covered with the lipid bilayers was placed in a variable angle ATR unit (Harrick, NY). To obtain hydrated bilayers, the germanium crystal was covered with a thermoregulated stainless steel recess jacket fitted with holes allowing liquid circulation above the ATR crystal. The clean and dry ATR crystal was first heated to 65°C and the SUV solution of DMPA (~1 ml) was introduced into the thermoregulated cell for 10 min. The temperature was then cooled down to room temperature for an additional 10 min. Approximately 10 ml of pure water was gently introduced into the cell to eliminate the excess of lipids and to keep the bilayers hydrated on each side of the ATR plate.

All spectral manipulations were performed with the SpectraCalc software (Galactic Industries Corp., Salem, NH). The spectra in the CH stretching mode region (3050–2750 cm^{-1}) were first baseline-corrected using either a linear function in the case of the spectra of the dry bilayers or a quadratic function in the case of the spectra of the hydrated bilayers. The baseline corrected spectra were then interpolated with one level of zero filling to better define the band maxima. Since the CH stretching mode region is composed of several overlapping bands, the dichroic ratio of the 2850 and 2918 cm^{-1} bands were calculated from the height of the bands at the maximum intensity. Band-fitting of the whole CH stretching mode region did not decrease the error on the determination of the dichroic ratio.

RESULTS AND DISCUSSION

Preparation of dry and hydrated single DMPA bilayers

The preparation of a single lipid bilayer is not straightforward. A well known method is the Langmuir-Blodgett (LB) technique because it allows control of the number and the surface density of the lipid layers. Because of the hydrophilic nature of the germanium crystal used in this study, the first DMPA monolayer was easy to transfer with the LB technique. However, the deposition of the second monolayer was not possible because the first monolayer was always retransferred back on the surface of the Langmuir trough when the covered substrates were immersed in the subphase. Other groups have reported similar redeposition problems with phospholipids (Lotta et al., 1988; Fringeli and Günthard, 1981; Hasmonay et al., 1979; Cui et al., 1990).

Fringeli et al. (1989) have proposed a method for the preparation of a supported single bilayer which consists of depositing a first monolayer by the LB method while the second monolayer is self-deposited by immersing the covered substrate in an SUV solution. Good results were obtained for DMPA using this method. Indeed, we have observed that the absorbance of the bands in the ATR spectra of a bilayer is twice that of a monolayer deposited in the liquid-condensed state by the LB technique with a transfer ratio of 1.0. Identical results were also obtained with a simpler method that has often been used for NMR measurements of phospholipid bilayers on spherical solid supports (Bayerl and Bloom, 1990; Picard et al., 1998). This technique, described in the Materials and Methods section, consists of immersing clean germanium crystals directly into an SUV solution.

Polarized attenuated total reflection of a DMPA bilayer

S and p-polarized ATR spectra of a dry and of a hydrated single DMPA bilayer deposited on each side of a germanium ATR crystal are shown in Fig. 1 for the 3050–2750 cm^{-1} region. Four bands can easily be distinguished: the antisymmetric CH_3 stretching band ($\nu_a(CH_3)$) at 2959 cm^{-1}, the antisymmetric CH_2 stretching band ($\nu_a(CH_2)$) at 2918 cm^{-1}, the symmetric CH_3 stretching band ($\nu_s(CH_3)$) at 2870 cm^{-1}, and the symmetric CH_2 stretching band

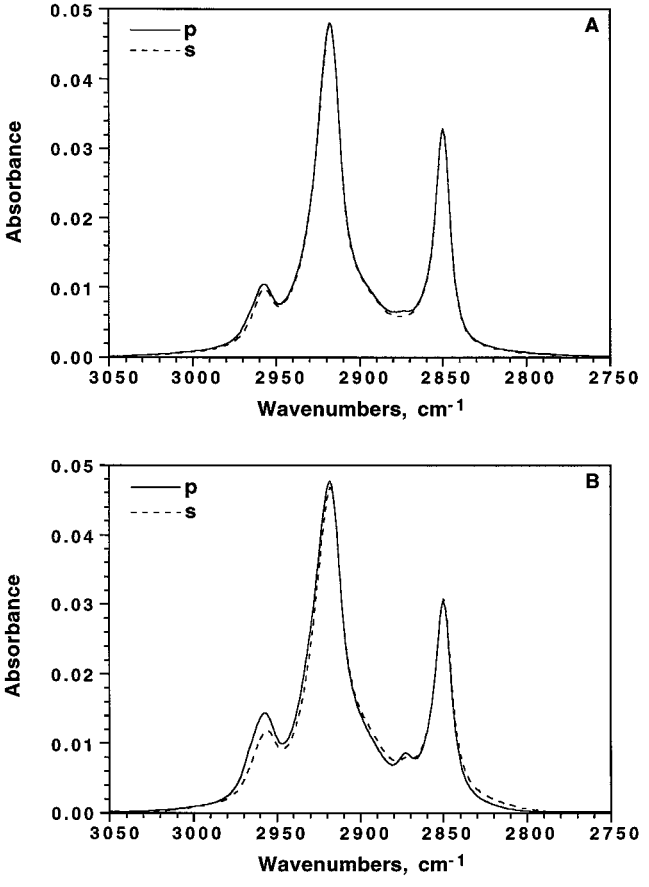

FIGURE 1 S and p-polarized ATR spectra of (*A*) dry and (*B*) hydrated single bilayers of DMPA deposited on each side of a germanium crystal.

($\nu_s(CH_2)$) at 2850 cm^{-1}. The position of the maximum of the methylene bands clearly indicates that both the dry and hydrated films are well ordered with the acyl chains in the all-*trans* conformation as observed for phospholipid dispersions in the gel phase (Mendelsohn and Mantsch, 1986; Mantsch and McElhaney, 1991). The close examination of these bands reveals that they are slightly broader in the spectra of the hydrated bilayers (by ~4 and 2 cm^{-1} for the 2918 and 2850 cm^{-1}, respectively), suggesting that the acyl chains of DMPA are more mobile in the hydrated film (Casal and Mantsch, 1984; Mantsch and McElhaney, 1991). The absorbance of the 2918 and 2850 cm^{-1} bands for both polarization states is 0.048 and 0.033 for the dry bilayers, respectively, which is twice that observed by Labrecque (1995) for a dry DMPA monolayer deposited on a germanium crystal by the LB method at a surface pressure of 20 mN/m. For the hydrated bilayers, the maximum intensity of the methylene bands is very close to that of the dry bilayer. However, the bands associated with the antisymmetric and symmetric CH_3 stretching vibrations at 2959 and 2870 cm^{-1}, respectively, are stronger in the ATR spectrum recorded with the infrared radiation polarized in the plane of incidence, suggesting that the acyl chains are less tilted in the hydrated film.

To determine the orientation of the acyl chain with respect to the normal to the ATR crystal, the dichroic ratio, R_{ATR}, was calculated from the polarized spectra of Fig. 1, using the following equation:

$$R_{ATR} = \frac{A_p}{A_s} \tag{21}$$

where A_p and A_s are the absorbances of the bands obtained with the infrared radiation polarized parallel and perpendicular to the plane of incidence, respectively. Highly reproducible dichroic ratios were obtained for four different dry and hydrated samples. For the dry bilayers, dichroic ratios of 1.00 ± 0.01 were calculated for both the 2918 and 2850 cm^{-1} methylene bands, while for the hydrated bilayers, dichroic ratios of 1.02 ± 0.02 and 1.00 ± 0.02 were obtained for these bands, respectively. The lower accuracy for the results obtained for the hydrated bilayers is essentially a result of the difficulty in eliminating the water contribution in the ATR spectra.

Assuming a uniaxial distribution of orientation of the acyl chains with respect to the normal to the ATR crystal (*z* axis), the order parameter, S_z, of the transition moment of a given vibration can be calculated from the three mean-square orthogonal electric field amplitudes, $\langle E^2_{x,y,z}\rangle$, using the following equation (Fringeli and Günthard, 1981):

$$S_z = \frac{\langle E^2_x\rangle - \langle E^2_y\rangle R_{ATR} + \langle E^2_z\rangle}{\langle E^2_x\rangle - \langle E^2_y\rangle R_{ATR} - 2\langle E^2_z\rangle}. \tag{22}$$

For acyl chains with cylindrical symmetry, the order parameter of the chain axis, $\langle P_2(\cos\theta)\rangle$, can be calculated from the order parameter of the transition moment, S_z, using the Legendre addition theorem:

$$\langle P_2(\cos\theta)\rangle = \frac{3\langle\cos^2\theta\rangle - 1}{2} = \frac{S_z}{P_2(\cos\beta)} \tag{23}$$

where θ is the angle between the acyl chain axis and the normal to the ATR crystal, and β is the angle between the transition moment and the acyl chain axis. In the case of the $\nu_a(CH_2)$ and $\nu_s(CH_2)$ vibrations, β is equal to 90° if the acyl chains are in the all-*trans* conformation. If the orientation distribution of the acyl chains is infinitely narrow, it is possible to calculate the tilt angle θ from Eq. 23 (Lafrance et al., 1995).

Equation 22 shows clearly that it is very important to accurately know the mean-square electric field amplitudes along the *x*, *y*, and *z* axis to perform orientation measurements by ATR spectroscopy. Since the mean-square electric field amplitudes depend on the film thickness as well as on the refractive indexes of the ATR crystal, film, and environment, it is important to use proper values for these parameters. The refractive index of germanium is equal to 4.0 and is fairly independent of the wavelength in the infrared region (Palik, 1985). The complex refractive index of water in the infrared region has recently been accurately determined by Bertie and Lan (1996). To our knowledge, the infrared dependence of the complex refractive indexes of phospholipid bilayers have not yet been published. We have thus determined these parameters for a DMPA bilayer, as described in the following section.

Determination of the optical constants for a bilayer of DMPA

To determine the optical constants of thin films using the procedure described in the Theory section, it is first necessary to know the thickness (*d*) and the refractive index of the film. The value used in this study for the thickness of a bilayer of DMPA is 40 Å, as determined by x-ray crystallography (Harlos et al., 1984). In the literature, values for the real refractive index of phospholipids of 1.4 (Citra and Axelsen, 1996), 1.44 (Brauner et al., 1987), and 1.5 (Frey and Tamm, 1991) have been used. Moreover, spectroscopic ellipsometry measurements on thin films of dimyristoylphosphatidylcholine have shown that the refractive index at 3000 cm^{-1} is 1.46 (D. Blaudez, unpublished results). In this study we have thus used a value of 1.45 for the refractive index of DMPA. The in-plane ($n_x = n_y$ and $k_x = k_y$) and out-of-plane (n_z and k_z) optical constants determined from the s- and p-polarized ATR spectra of the dry DMPA bilayers, respectively, are presented in Fig. 2 for the 3050–2750 cm^{-1} region. The values of the refractive index and the extinction coefficient at 2918 and 2850 cm^{-1} are reported in Table 1. The higher values of the in-plane extinction coefficient compared to the out-of-plane values for the methylene bands clearly confirm that the film is anisotropic and that the transition moments of the methylene stretching vibrations are rather parallel to the surface.

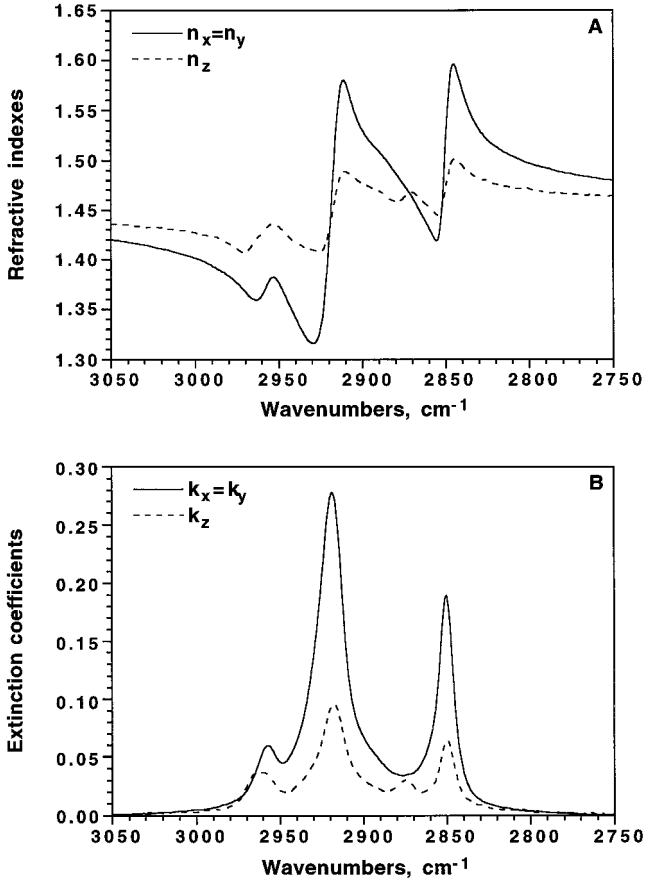

FIGURE 2 (*A*) Anisotropic refractive indexes ($n_x = n_y$ and n_z) and (*B*) extinction coefficients ($k_x = k_y$ and k_z) of DMPA determined from the s- and p-polarized ATR spectra of the dry single DMPA bilayers.

From the values of the extinction coefficients along the *x*, *y*, and *z* directions for a given absorption band, it is possible to calculate the maximum extinction coefficient, k_{max}, when all transition moments are oriented along the same direction and the isotropic extinction coefficient, k_{iso}, when the transition moments are randomly oriented, using the following equation:

$$k_{max} = k_x + k_y + k_z = 3k_{iso}. \quad (24)$$

The value of k_{max} that depends on the strength of the oscillator and the molecular density of the film is 0.652 and 0.443 at the maximum intensity of the 2918 and 2850 cm^{-1} bands, respectively (Table 1). A k_{max} of 1.07 for the 2918 cm^{-1} band has recently been determined by Flach et al. (1997) for a condensed monolayer film of behenic acid methyl ester (BAME) at the air-water interface. The value of k_{max} per methylene group being 0.053 for BAME and 0.050 DMPA suggests that the difference between the k_{max} for the two systems is essentially due to the difference in the number of methylene groups, and that the packing surface density of the methylene groups is essentially the same in the two systems.

TABLE 1 Values of the anisotropic optical constants of a DMPA bilayer at 2918 and 2850 cm^{-1}

	$n_x = n_y$	n_z	$k_x = k_y$	k_z	k_{max}
2918 cm^{-1}	1.470	1.446	0.278	0.096	0.652
2850 cm^{-1}	1.487	1.472	0.189	0.065	0.443

Determination of the mean-square electric field amplitudes

The electric field amplitudes along the *x*, *y*, and *z* axes were calculated using the formalism described in the Theory section for an isotropic three-phase system. The isotropic optical constants at 2918 cm^{-1} of germanium, DMPA, and water used in these calculations are given in Table 2. Fig. 3 shows the effect of the film thickness, up to 2 μm, on the three calculated orthogonal mean-square electric field amplitudes in a dry DMPA bilayer, at the interface between the film and the ATR crystal (initial values), for a nonabsorbing film ($k = 0$) and for an absorbing film ($k = 0.217$). As predicted from the Harrick equations, the electric field amplitude along the *z* direction is much more sensitive to the film thickness than those along the *x* and *y* directions. The three electric fields change up to $\sim$1 μm and then remain constant. For a nonabsorbing film, $\langle E_z^2 \rangle$ increases from an initial value of 0.515 to a maximum value of 2.651. However, for the same thickness range, $\langle E_x^2 \rangle$ decreases only from 1.991 to 1.954 while $\langle E_y^2 \rangle$ increases from 2.133 to 2.303. As seen in this figure, the limiting values of the electric field amplitudes are in perfect agreement with those calculated from the Harrick approximate equations for thin and thick films. However, for film thicknesses between 0 and 0.5 μm, the Harrick equations do not allow the accurate calculation of the mean-square electric fields. In addition, Figure 3 shows that for thick absorbing films, the electric field amplitudes calculated from the thickness-dependent formalism differ significantly from those calculated from the approximate Harrick equations, revealing the limitations of these equations. All initial values of the three electric field amplitudes are smaller for the absorbing film than those calculated for the nonabsorbing film.

The results of Figure 3 clearly show that it is important to consider both the film thickness and the extinction coefficient of the studied film to precisely determine the initial values of the three electric field amplitudes. However, it is also important to know the variation of the mean-square electric field amplitudes as a function of the depth in the film. Fig. 4 shows this variation for a 40-Å absorbing dry

TABLE 2 Values of the isotropic optical constants of germanium, DMPA bilayer, and water at 2918 cm^{-1} used in the calculation of the electric field amplitudes

	n	k_{iso}
Germanium	4.0	0.0
DMPA	1.45	0.217
Water	1.42	0.0155

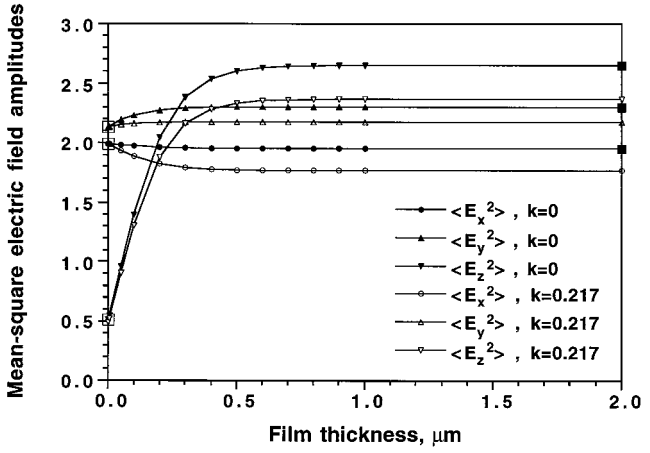

FIGURE 3 Effect of the film thickness on the three calculated orthogonal mean-square electric field amplitudes, $\langle E_i^2 \rangle$, in a dry DMPA bilayer, at the interface between the film and the ATR crystal (initial values), for nonabsorbing film ($k = 0$) and absorbing films ($k = 0.217$). The open and filled squares are the values calculated using the Harrick thin and thick film equations, respectively.

DMPA bilayer. As can be seen, even for an ultra-thin film, the electric field amplitudes are not constant throughout the film, $\langle E_x^2 \rangle$, $\langle E_y^2 \rangle$ and $\langle E_z^2 \rangle$ decreasing by ~2, 4, and 8%, respectively. Therefore, the error made in orientation measurements by using the initial values of the electric field amplitudes is not negligible, especially for the field along the *z* direction. The use of the mean values of the electric field amplitudes over the film thickness should be more appropriate. The initial and mean values of the mean-square electric field amplitudes are compared in Table 3 for an absorbing ($k = 0.217$) dry DMPA bilayer with a thickness of 40 Å.

Finally, the mean-square electric field amplitudes for the two-phase approximation, where the film is not considered, have also been calculated and the values obtained are presented in Table 3. $\langle E_x^2 \rangle$ and $\langle E_y^2 \rangle$ have values similar to those obtained using approximate Harrick thin film equations, whereas $\langle E_z^2 \rangle$ is much stronger because the two-phase approximation does not take into account the refractive index of the film.

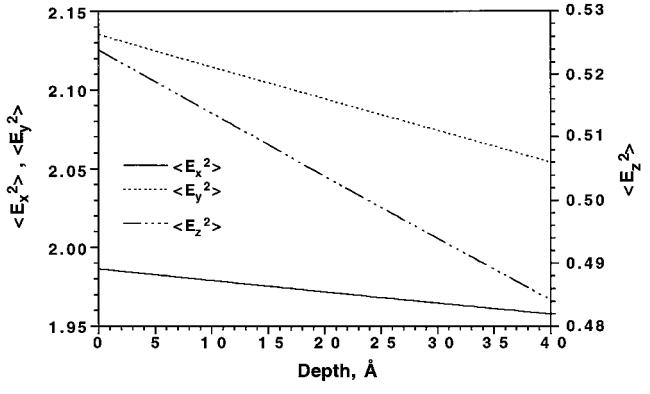

FIGURE 4 Effect of the depth of penetration on the three calculated orthogonal mean-square electric field amplitudes, $\langle E_i^2 \rangle$, in a 40 Å thick dry DMPA bilayer.

The mean-square electric field amplitudes along the *x*, *y*, and *z* directions have also been calculated for a hydrated DMPA bilayer using the different models described above for the dry film, and are presented in Table 3. As can be seen, the change of $\langle E_z^2 \rangle$ with the film thickness is drastically reduced when the DMPA bilayer is covered with water and the value of $\langle E_z^2 \rangle$ is nearly independent of the model used for the calculation of the electric fields. This effect is essentially due to the fact that the refractive index of water is very close to that of the phospholipid (Table 2).

From the values of the mean-square electric field amplitudes calculated using the different models and the experimental dichroic ratios of dry and hydrated DMPA bilayers, the order parameter, $\langle P_2 (\cos \theta) \rangle$, and the average tilt angle, $\langle \theta \rangle$, of the acyl chains have been calculated using Eqs. 22 and 23, and are presented in Table 3. For the dry bilayer, the tilt angle ranges from 28 to 30°, except for the two-phase approximation that gives a tilt angle of 14°; for the hydrated bilayer, however, the tilt angle is always between 22 and 23°, no matter which model is used to calculate the electric fields.

Because the different models for the calculations of the electric fields give different results for the acyl chain tilt angle for a dry DMPA bilayer, it is important to determine which model is the best one. For that purpose, s- and p-polarized ATR spectra of a 40-Å lipid layer were simulated for different molecular tilt angles. For each spectrum simulated with a given tilt angle ("real tilt angle"), we have calculated the dichroic ratio and the associated order parameter and tilt angle ("calculated tilt angle") using the different sets of electric fields given in Table 3. Finally, the difference between the real and the calculated tilt angles has been analyzed to determine which set of electric fields gives the best results.

Effect of the acyl chain tilt angle on the dichroic ratio

To simulate the polarized ATR spectra of a thin phospholipid film, we have used a single Lorentzian band centered at 2918 cm^{-1} with a maximum extinction coefficient $k_{max} = 0.652$ and a width at half-height of 18 cm^{-1}. These parameters are typical of the band due to the antisymmetric methylene stretching vibration in the DMPA spectra. For each tilt angle, θ, the extinction coefficients k_x, k_y, and k_z were calculated from k_{max} using the following equations (Fraser and MacRea, 1973), assuming that the symmetry of orientation of the acyl chains is uniaxial and that the angle between the transition moment and the chain axis, β, is 90°:

$$k_x = k_y = \left[\frac{1 + \cos^2\theta}{4}\right] \cdot k_{max} \quad (25)$$

$$k_z = \left[\frac{1 - \cos^2\theta}{2}\right] \cdot k_{max}. \quad (26)$$

TABLE 3 Values of the mean-square electric field amplitudes at 2918 cm^{-1}, acyl chain order parameter, and tilt angle calculated with different formalisms for a dry and a hydrated bilayer of DMPA in ATR infrared spectroscopy

	$\langle E_x^2 \rangle$	$\langle E_y^2 \rangle$	$\langle E_z^2 \rangle$	$\langle P_2(\cos\theta) \rangle^{\|}$	$\langle \theta° \rangle$**
Dry bilayer of DMPA, $R_{ATR} = 1.00$					
Harrick thin film*	1.991	2.133	0.515	0.637	29.5
Two-phase approximation#	1.991	2.133	2.276	0.909	14.2
Thickness- and absorption-dependent					
Initial values§	1.987	2.135	0.524	0.629	29.8
Mean values¶	1.972	2.095	0.504	0.674	27.8
Hydrated bilayer of DMPA, $R_{ATR} = 1.02$					
Harrick thin film*	1.958	2.288	2.408	0.783	22.4
Two-phase approximation#	1.958	2.288	2.618	0.799	21.5
Thickness- and absorption-dependent					
Initial value§	1.938	2.276	2.391	0.777	22.7
Mean values¶	1.908	2.236	2.350	0.780	22.5

*Calculated for a nonabsorbing and infinitely thin film ($d = 0$), using Eqs. 16–18.
#The film is not considered; calculated using Eqs. 12–14.
§Initial values of the electric field amplitudes in an absorbing film ($k = 0.217$) of 40 Å thickness.
¶Mean values of the electric field amplitudes in an absorbing film ($k = 0.217$) of 40 Å thickness.
‖Calculated using Eq. 22 with $\beta = 90°$.
**Calculated using Eq. 23, considering an infinitely narrow distribution of orientation.

The refractive indexes along the *x*, *y*, and *z* directions were calculated by the Kramers-Kronig transformation of the corresponding extinction coefficients, using $n = 1.45$. The s- and p-polarized ATR spectra were then simulated using the formalism described in the Theory section, and the dichroic ratio was determined from these spectra.

Fig. 5 shows the dependence of the dichroic ratio on the tilt angle for the 0–40° range for both the dry and hydrated films. This range of angles has been chosen since lipid acyl chains tend to orient rather vertically with respect to the ATR crystal. As can be seen in Fig. 5, the variation of the dichroic ratio with the tilt angle is more important for the hydrated film than for the dry film. This is due to the fact that in the hydrated film, $\langle E_z^2 \rangle$ is ~5 times higher than in the dry film, allowing a better sensitivity for the determination of the orientation of the acyl chains. Furthermore, the variation of the dichroic ratio for tilt angles below 15° is very small. It can thus be concluded that the ATR bands resulting from the methylene stretching vibrations are not suitable for precise orientation measurements of acyl chains with tilt angles <15°. In such a case, vibrations with transition moment parallel to the chain axis, such as the wagging progression vibrations, should be used (Brauner et al., 1987; Ahn and Franses, 1992). Fig. 5 also stresses the importance of determining the dichroic ratio with the highest possible accuracy. For DMPA, the dichroic ratio determined experimentally for the 2918 cm^{-1} band is 1.00 ± 0.01 for the dry film and 1.02 ± 0.02 for the hydrated film, giving tilt angles of 28 ± 2° and 23 ± 2°, respectively. Nevertheless, the results obtained for the dry film show that the chain tilt angle in the DMPA bilayers is close to the 31° value determined by x-ray diffraction on crystalline DMPA (Harlos et al., 1984).

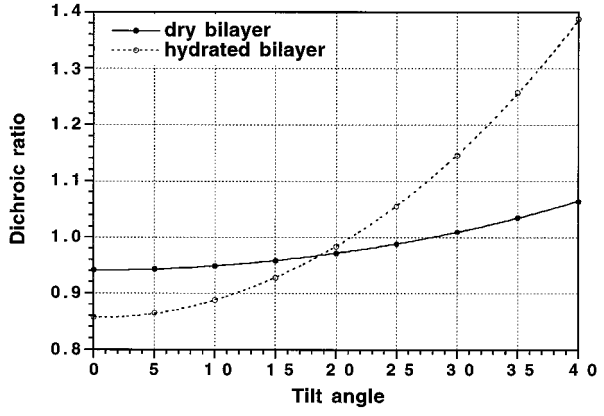

FIGURE 5 Effect of the acyl chain tilt angle on the dichroic ratio obtained from the simulated ATR spectra of both dry and hydrated 40-Å-thick lipid bilayers for a vibration with a transition moment perpendicular to the chain axis.

Validity of the different models used to calculate the mean-square electric fields

Fig. 6 shows the correlation between the tilt angle calculated from the dichroic ratio and the real tilt angle in the 0–40° range for the different models used to calculate the mean-square electric fields for dry and hydrated 40-Å lipid films. The results presented in Fig. 6 *A* for the dry film indicates that the Harrick thin film equations give overestimated tilt angles, the difference between the real and calculated tilt angles increasing as the tilt angle decreases. For example, the error made by using the Harrick equations is only 2° at a tilt angle of 25°, but it is 10° for a tilt angle of 0°. As seen in Fig. 6 *A*, the results obtained using the initial values of the mean-square electric fields calculated using the thickness- and absorption-dependent formalism are not better than

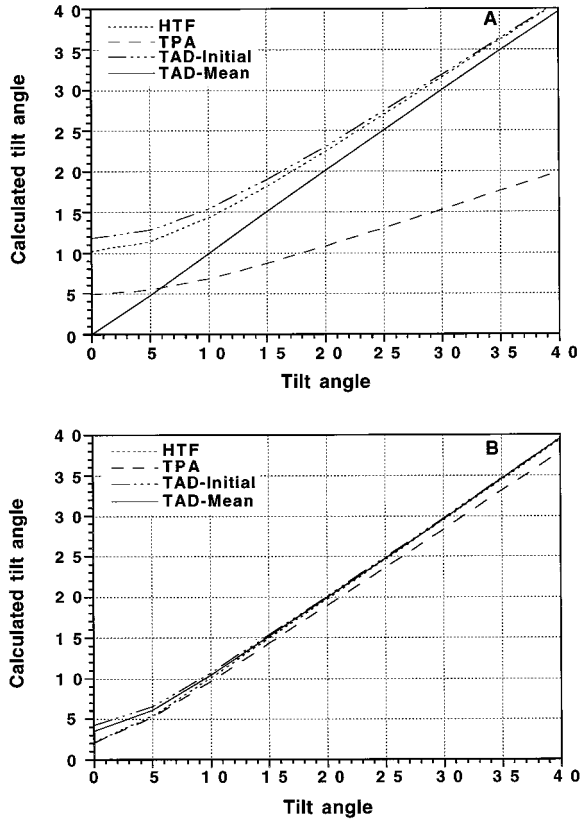

FIGURE 6 Correlation between the "calculated" and "real" acyl chain tilt angles for (*A*) a dry and (*B*) a hydrated 40-Å-thick lipid bilayer using electric field amplitudes obtained from the Harrick thin film equations (HTF), from the thickness- and absorption-dependent formalism using initial (TAD-Initial) and mean (TAD-Mean) values, and from the two-phase approximation (TPA).

those obtained from the Harrick thin films equations. However, when the mean values of the electric fields over the film thickness (see Table 3) are used to calculate the tilt angle, the thickness- and absorption-dependent formalisms give calculated tilt angles that are in almost perfect agreement with the real ones. Finally, it is clear from Fig. 6 *A* that the two-phase approximation is not adequate for the determination of the chain orientation in phospholipid thin films in air.

These results show unambiguously that to obtain accurate values of acyl chain tilt angles in dry lipid films, it is important to use the more complete model to calculate the electric fields, such as the thickness- and absorption-dependent one, using the mean values of the electric field over the film thickness. However, such a model is not straightforward to use routinely, and the Harrick thin film approximation provides acceptable results for very thin films ($d < 40$ Å) where the variation of the electric fields over the film thickness is relatively small, and for tilt angle $>15°$. When the lipid film is covered with water (Fig. 6 *B*), however, all models give reasonably good correlations between the calculated and real tilt angles. This results from the fact that for the hydrated lipid film, the mean-square electric field amplitudes are nearly independent of the model used for the calculation (see Table 3).

Factors affecting the orientation measurements

Several factors may affect the accuracy of an orientation measurement done by ATR spectroscopy. Some of them are related to physical characteristics of the studied system, such as the refractive index and the thickness of the film, and others are related to the definition of the system itself, such as the width of the orientation distribution and the symmetry of the system.

Values of the real refractive index of phospholipids between 1.4 and 1.5 have been used in the literature (Citra and Axelsen, 1996; Frey and Tamm, 1991; Brauner et al., 1987). Fig. 7 shows the effect of the refractive index on the determination of the tilt angle. For the observed dichroic ratio of the dry DMPA bilayer ($R_{ATR} = 1.00$), the tilt angle increases from 26° for $n = 1.4$ to 30° for $n = 1.5$. The effect of the refractive index on the determination of the tilt angle increases with the tilt angle. However, for tilt angles $<30°$, which is the case for most phospholipids, the change of the tilt angle for refractive indexes between 1.4 and 1.5 is approximately the same as that due to the experimental error on the determination of the dichroic ratio, as seen in Fig. 7.

It has been shown above that the film thickness is important in the calculation of electric field amplitudes. Fig. 8 shows the effect of the film thickness on the determination of the tilt angle. Calculations were done for a single monolayer (20 Å), a single bilayer (40 Å), and a 60-Å thick film. As seen in this figure, for a dichroic ratio of 1.00, increasing the film thickness by a factor of three from 20 to 60 Å results in a change of the tilt angle of only 2°. This change in the tilt angle is lower than the error because of the experimental uncertainty of the determination of the dichroic ratio. Therefore, in the case of ultra-thin films of lipids, such as monolayers or bilayers, it is not necessary to precisely determine the film thickness to determine chain tilt angles. However, for film thicknesses between 200 Å

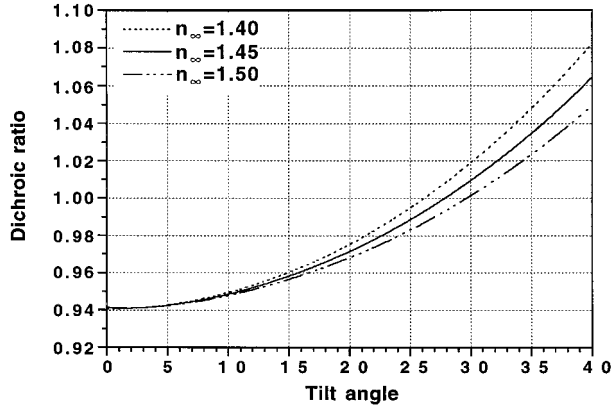

FIGURE 7 Effect of the lipid refractive index on the dichroic ratio obtained from the simulated ATR spectra of a dry lipid bilayer for a vibration with a transition moment perpendicular to the chain axis.

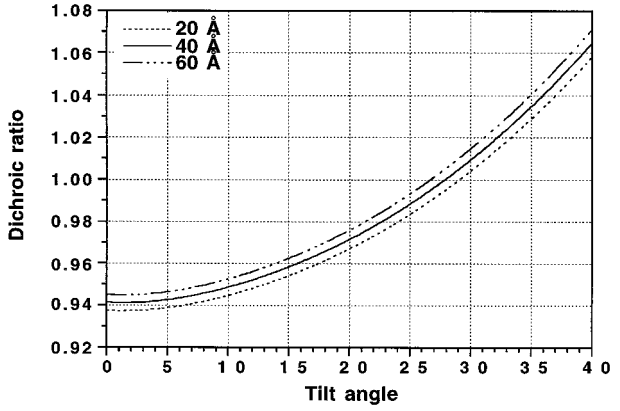

FIGURE 8 Effect of the film thickness on the dichroic ratio obtained from the simulated ATR spectra of a dry lipid film for a vibration with a transition moment perpendicular to the chain axis.

and 0.5 μm, the results of Fig. 3 clearly show that the film thickness has to be known precisely for reliable orientation measurements by ATR spectroscopy. In this case it is necessary to use the thickness- and absorption-dependent formalism to determine the mean-square electric field amplitudes.

In addition to these physical factors that have an effect on the determination of the mean-square electric field amplitudes, the presence of surface irregularities of the ATR crystal (Axelsen et al., 1995a) and of conformational disorder along the lipid acyl chains (Lafrance et al., 1995) result in the broadening of the orientation distribution and in errors in the determination of the tilt angle. Furthermore, it is often assumed that the symmetry of orientation is cylindrical around the molecular axis and that the distribution of orientation of the investigated system is uniaxial. These two hypotheses are not valid for certain protein conformations, such as the β-sheets, (Marsh, 1997) and for phospholipids in the subgel phase (Nagle, 1993; LeBihan and Pézolet, 1998) where the symmetry of the chain axis is not cylindrical. In addition, the orientation of a transition moment relative to the molecular axis is not always precisely known. For example, in the case of the α-helix, values between 24 and 39° have been used in the literature for the angle between the transition moment of the amide I vibration and the helix axis (Tsuboi, 1962; Rothschild and Clark, 1979; Axelsen et al., 1995a). Finally, in the case of a heterogeneous system, such as lipid-protein complexes, a macroscopic approach to calculating the molecular orientation may not be appropriate. These factors may explain why the Harrick thin film approximation failed to give reliable molecular orientation results for certain systems.

CONCLUSION

Polarized ATR spectroscopy is a powerful method for studying the molecular orientation of axially symmetric films. In this study we have compared different formalisms for the calculation of the mean-square electric field amplitudes, such as the Harrick thin film approximation, the two-phase approximation, and the general thickness- and absorption-dependent model for lipid films. In the case of ultra-thin films of lipids, such as monolayers or bilayers, the orientation of the acyl chain axis can be determined with reasonable accuracy using the Harrick thin film equations. However, for films thicker than 200 Å, it is necessary to use the more elaborate formalism that takes into account both the thickness and the absorption of the film. However, the two-phase approximation, where the film is neglected, is not adequate for the determination of the chain orientation in dry phospholipid thin films. Spectral simulations of the lipid methylene stretching vibrations indicate that the change of the dichroic ratio with the chain tilt angle is more pronounced when the film is covered with water, compared to the dry film. In addition, for hydrated films, all formalisms used to calculate the mean-square electric field amplitudes give good results. Finally, this study clearly shows that uncertainty of the determination of the tilt angle comes mostly from the experimental error on the dichroic ratio and from the knowledge of the refractive index.

The authors are grateful to Prof. John E. Bertie of the University of Alberta for providing data on the complex refractive index of water.

This work was supported by the Natural Science and Engineering Research Council (NSERC) of Canada, by the Fonds pour la Formation de Chercheurs et pour l'Aide à la Recherche (FCAR) from the Province of Quebec, and by the Conseil National de la Recherche Scientifique (France). We also thank NSERC for the award of a postgraduate scholarship (to F.P.).

REFERENCES

Abelès, F. 1967. Optics of thin films. *In* Advanced Optical Techniques. North Holland, Amsterdam. 143–188.

Ahn, D. J., and E. I. Franses. 1992. Orientation of chain axes and transition moments in Langmuir-Blodgett monolayers determined by polarized FTIR-ATR spectroscopy. *J. Phys. Chem.* 96:9952–9959.

Allara, D. L., and J. D. Swallen. 1982. An infrared reflection spectroscopy study of oriented cadmium arachidate monolayer films on evaporated silver. *J. Phys. Chem.* 86:2700–2704.

Axelsen, P. H., W. D. Braddock, H. L. Brockman, C. M. Jones, R. A. Dluhy, B. K. Kaufmann, and F. J. Puga II. 1995b. Use of the internal reflectance infrared spectroscopy for the in-situ study of supported lipid monolayers. *Appl. Spectrosc.* 49:526–531.

Axelsen, P. H., and M. Citra. 1997. Orientational order determination by internal reflection infrared spectroscopy. *Prog. Biophys. Mol. Biol.* 66: 227–253.

Axelsen, P. H., B. K. Kaufman, R. N. McElhaney, and R. N. A. H. Lewis. 1995a. The infrared dichroism of transmembrane helical polypeptides. *Biophys. J.* 69:2770–2781.

Baenziger, J. E., K. W. Miller, and K. J. Rothchild. 1992. Incorporation of nicotinic acetylcholine receptor into planar multilamellar films: characterization by fluorescence and Fourier transform infrared difference spectroscopy. *Biophys. J.* 51:983–992.

Bayerl, T. M., and M. Bloom. 1990. Physical properties of single phospholipid bilayers adsorbed to microglass beads: a new vesicular model system studied by ^{2}H-nuclear magnetic resonance. *Biophys. J.* 58: 357–362.

Bertie, J. E., and Z. Lan. 1996. Infrared intensities of liquids XX: the intensity of the OH stretching band of liquid water revisited, and the best current values of the optical constants of H_2O (l) at 25°C between 15,000 and 1 cm^{-1}. *Appl. Spectrosc.* 50:1047–1057.

Blaudez, D., T. Buffeteau, J. C. Cornut, B. Desbat, N. Escafre, M. Pézolet, and J. M. Turlet. 1993. Polarization-modulated FT-IR spectroscopy of

spread monolayer at the air/water interface. *Appl. Spectrosc.* 47: 869–874.

Blaudez, D., T. Buffeteau, B. Desbat, P. Fournier, A. M. Ritcey, and M. Pézolet. 1998. Infrared reflection-absorption spectroscopy of thin organic films on nonmetallic substrates: optimal angle of incidence. *J. Phys. Chem. B.* 102:99–105.

Brandenburg, K., and U. Seydel. 1986. Orientation measurements on ordered multilayers of phospholipids and sphingolipids from synthetic and natural origin by ATR Fourier transform infrared spectroscopy. *Z. Naturforsch.* 41c:453–467.

Brauner, J. W., R. Mendelsohn, and F. G. Prendergast. 1987. Attenuated total reflectance Fourier transform infrared studies of the interaction of melittin, two fragments of melittin, and δ-hemolysin with phosphatidylcholines. *Biochemistry.* 26:8151–8158.

Buffeteau, T., B. Desbat, E. Péré, and J. M. Turlet. 1997. Determination of the optical constants in a uniaxial film from FT-IR spectroscopy. *Mikrochim. Acta.* 14:631–633.

Buffeteau, T., B. Desbat, and J. M. Turlet. 1991. Polarization modulation FT-IR spectroscopy of surfaces and ultra-thin films: experimental procedure and quantitative analysis. *Appl. Spectrosc.* 45:380–389.

Casal, H. L., and H. H. Mantsch. 1984. Polymorphic phase behavior of phospholipid membranes studied by infrared spectroscopy. *Biochim. Biophys. Acta.* 779:381–401.

Chollet, P. A., and J. Messier. 1982. Studies of oriented Langmuir-Blodgett multilayers by infrared linear dichroism. *Chem. Phys.* 73:235–242.

Citra, M. J., and P. H. Axelsen. 1996. Determination of molecular order in supported lipid membranes by internal reflection Fourier transform infrared spectroscopy. *Biophys. J.* 71:1796–1805.

Cornell, D. G., R. A. Dluhy, M. S. Briggs, C. J. McKnight, and L. M. Gierash. 1989. Conformation and orientation of a signal peptide interacting with phospholipid monolayers. *Biochemistry.* 28:2789–2797.

Cropek, D. M., and P. H. Bohn. 1990. Surface molecular orientations determined by electronic linear dichroism in optical waveguide structures. *J. Phys. Chem.* 94:6452–6457.

Cui, D. F., V. A. Howarth, M. C. Petty, H. Ancelin, and J. Yarwood. 1990. The deposition and characterization of phosphatidic acid Langmuir-Blodgett films. *Thin Solid Films.* 192:291–296.

Flach, C. R., A. Gericke, and R. Mendelsohn. 1997. Quantitative determination of molecular chain tilt angles in monolayer films at the air/water interface: infrared reflection/absorption spectroscopy of behenic acid methyl ester. *J. Phys. Chem.* 101:58–65.

Fraser, R. D. B., and T. P. MacRea. 1973. The alpha-helix. *In* Conformation of Fibrous Proteins and Related Synthetic Polypeptides. Academic Press, New York. 179–217.

Frey, S., and L. K. Tamm. 1991. Orientation of melittin in phospholipid bilayers: a polarized attenuated total reflection study. *Biophys. J.* 60: 922–930.

Fringeli, U. P., H. J. Apell, M. Fringeli, and P. Laüger. 1989. Polarized infrared absorption of Na^+/K^+-ATPase studied by attenuated total reflection spectroscopy. *Biochim. Biophys. Acta.* 984:301–312.

Fringeli, U. P., and H. H. Günthard. 1981. Infrared membrane spectroscopy. *In* Membrane Spectroscopy. E. Grell, editor. Springer-Verlag, New York. 270–332.

Golden, M. G., D. S. Dunn, and J. Overend. 1981. A method for measuring infrared reflection-absorption spectra of molecules absorbed on low-area surfaces at monolayer and submonolayer concentrations. *J. Catalysis.* 71:395–404.

Goormaghtigh, E., V. Cabiaux, and J. M. Ruysschaert. 1990. Secondary structure and dosage of soluble and membrane proteins by attenuated total reflection Fourier-transform infrared spectroscopy on hydrated films. *Eur. J. Biochem.* 193:409–420.

Hansen, W. H. 1965. Expanded formulas for attenuated total reflection and the derivation of absorption rules for single and multiple ATR spectrometer cells. *Spectrochemica Acta.* 21:815–833.

Hansen, W. H. 1968. Electric fields produced by the propagation of plane coherent electromagnetic radiation in a stratified medium. *J. Opt. Soc. Am.* 58:380–390.

Hansen, W. H. 1972. Surface chemistry by reflection spectroscopy. *Prog. Nucl. Energy.* 11:3–35.

Hansen, W. H. 1973. Internal reflection spectroscopy in electrochemistry. *Adv. Electrochem. Electrochem. Eng.* 9:1–60.

Harlos, K., H. Eible, I. Pascher, and S. Sundell. 1984. Conformation and packing properties of phosphatidic acid: the crystal structure of monosodium dimyristoylphosphatidate. *Chem. Phys. Lipids.* 34:115–126.

Harrick, N. J. 1965. Electric field strengths at totally reflecting interfaces. *J. Opt. Soc. Am.* 55:851–857.

Harrick, N. J. 1967. Internal reflection spectroscopy. Harrick Scientific Corporation, Ossining, NY.

Hasmonay, H., M. Caillaud, and M. Dupeyrat. 1979. Langmuir-Blodgett multilayers of phosphatidic acid and mixed phospholipids. *Biochem. Biophys. Res. Commun.* 89:338–344.

Higashiyama, T., and T. Takenaka. 1974. Infrared attenuated total reflection spectra of adsorbed layers at the interface between a germanium electrode and an aqueous solution of sodium laurate. *J. Phys. Chem.* 78:941–947.

Jang, W.-H., and J. D. Miller. 1995. Molecular orientation of Langmuir-Blodgett and self-assembled monolayers of stearate species at a fluorite surface as described by linear dichroism theory. *J. Phys. Chem.* 99: 10272–10279.

Kimura, F., J. Umemura, and T. Takenaka. 1986. FTIR-ATR studies of Langmuir-Blodgett films of stearic acid with 1–9 monolayers. *Langmuir.* 2:96–101.

Labrecque, J. 1995. Étude par spectroscopie infrarouge de l'interaction de la polysine avec l'acide phosphatidique dans des films monomoléculaires. Mémoire de maîtrise. Université Laval, Québec, Canada.

Lafrance, C. P., A. Nabet, R. E. Prud'homme, and M. Pézolet. 1995. On the relationship between the order parameter $\langle P_2(\cos\theta)\rangle$ and the shape of the orientation distributions. *Can. J. Chem.* 73:1497–1505.

LeBihan, T., and M. Pézolet. 1998. Study of the structure and phase behavior of diplamitoylphosphatidylcholine by infrared spectroscopy: characterization of the pretransition and subtransition. *Chem. Phys. Lipids.* 94:13–33.

Lotta, T. I., L. J. Laakkonen, J. A. Virtanen, and P. K. J. Kinnunen. 1988. Characterization of Langmuir-Blodgett films of 1,2-dipalmitoyl-*sn*-glycero-3-phosphatidylcholine and 1-palmitoyl-2-[10-(pyren l-yl)decanoyl]-*sn*-glycero-3-phosphatidylcholine by FTIR-ATR. *Chem. Phys. Lipids.* 46:1–12.

Lukes, P. J., M. C. Petty, and J. Yarwood. 1992. An infrared study of the incorporation of ion channel forming peptides into Langmuir-Blodgett films of phosphatidic acid. *Langmuir.* 8:3043–3050.

Mantsch, H. H., and D. Chapman, editors. 1996. Infrared Spectroscopy of Biomolecules. Wiley, New York.

Mantsch, H. H., and R. N. McElhaney. 1991. Phospholipid phase transition in model and biological membranes as studied by infrared spectroscopy. *Chem. Phys. Lipids.* 57:213–226.

Marsh, D. 1997. Dichroic ratios in polarized Fourier transform infrared for nonaxial symmetry of β-sheet structures. *Biophys. J.* 72:2710–2718.

Mendelsohn, R., and H. H. Mantsch. 1986. Fourier transform infrared studies of lipid-protein interaction. *In* Progress in Lipid-Protein Interactions. A. Watts and J. J. H. H. M. De Pont, editors. Elsevier, Amsterdam.

Mirabella, F. J., and N. J. Harrick. 1985. Internal Reflection Spectroscopy: Review and Supplement. Harrick Scientific Corporation, Ossining, NY.

Nagle, J. F. 1993. Evidence of partial rotational order in gel phase DPPC. *Biophys. J.* 64:1110–1112.

Okamura, E., J. Umemura, and T. Takenaka. 1985. Fourier transform infrared-attenuated total reflection spectra of dipalmitoylphosphatidylcholine monomolecular films. *Biochim. Biophys. Acta.* 812:139–146.

Okamura, E., J. Umemura, and T. Takenaka. 1986. Orientation of gramicidin D incorporated into phospholipid multibilayers: a Fourier transform infrared-attenuated total reflection spectroscopic study. *Biochim. Biophys. Acta.* 856:68–75.

Palik, E. D. 1985. Handbook of Optical Constants of Solids. Academic Press, NY. 465–478.

Pascher, I., S. Sundell, K. Harlos, and H. Eibl. 1987. Conformation and packing properties of membrane lipids: the crystal structure of sodium dimyristoylphosphatidylglycerol. *Biochim. Biophys. Acta.* 896:77–88.

Picard, F., M. J. Paquet, E. J. Dufourc, and M. Auger. 1998. Measurement of the lateral diffusion of dipalmitoylphosphatidylcholine adsorbed on silica beads in the absence and presence of melittin: A ^{31}P 2D exchange solid-state NMR study. *Biophys. J.* 74:857–868.

Rabolt, J. F., F. C. Burns, N. E. Schlotter, and J. D. Swallen. 1983. Anisotropic orientation in molecular monolayers by infrared spectroscopy. *J. Chem. Phys.* 78:946–952.

Rothschild, K. J., and N. A. Clark. 1979. Polarized infrared spectroscopy of oriented purple membrane. *Biophys. J.* 25:473–487.

Subirade, M., C. Salesse, D. Marion, and M. Pézolet. 1995. Interaction of a wheat lipid transfer protein with phospholipid monolayers imaged by fluorescence microscopy and studied by infrared spectroscopy. *Biophys. J.* 69:974–988.

Takenaka, T., K. Harada, and M. Matsumoto. 1980. Structural studies of poly-γ-benzyl-L-glutamate monolayers by infrared ATR and transmission spectra. *J. Colloid. Interface Sci.* 73:569–577.

Tsuboi, M. 1962. Infrared dichroism and molecular conformation of α-form poly-γ-benzyl-L-glutamate. *J. Polym. Sci.* 59:139–153.

Umemura, J., T. Kamata, T. Kawai, and T. Takenaka. 1990. Quantitative evaluation of molecular orientation in thin Langmuir-Blodgett films by FTIR transmission and reflection-absorption spectroscopy. *J. Phys. Chem.* 94:62–67.

Van Dick, P. W. M., B. de Kruijff, A. J. Verkleij, L. L. M. Van Deenen, and J. de Gier. 1978. Comparative studies of the effects of pH and Ca^{2+} on bilayers of various negatively charged phospholipids and their mixtures with phosphatidylcholine. *Biochim. Biophys. Acta.* 512:84–96.

Vogel, H., F. Jahnig, V. Hoffmann, and J. Stumpel. 1983. The orientation of melittin in lipid membranes: a polarized infrared spectroscopy study. *Biochim. Biophys. Acta.* 733:201–209.

Yamamoto, K., and H. Ishida. 1994. Interpretation of reflection and transmission spectra for thin films: reflection. *Appl. Spectrosc.* 48:775–787.